

Examining the factors that govern the regioselectivity in rhodium-catalysed alkyne cyclotrimerisation

Òscar Torres, Martí Fernández, Àlex Díaz-Jiménez, Anna Pla-Quintana*, Anna Roglans and Miquel Solà*

Institut de Química Computacional i Catàlisi (IQCC) and Departament de Química, Universitat de Girona, C/ Maria Aurèlia Capmany, 69, E-17003, Girona, Catalonia, Spain, e-mail: anna.plaq@udg.edu; miquel.sola@udg.edu.

ABSTRACT: The electronic and steric factors that favour the formation of 1,2,4- and 1,3,5-regioisomers in the intermolecular [2+2+2] cyclotrimerisation of terminal alkynes are not well understood. In this work, this problem was analysed from a theoretical and experimental point of view. Density functional theory (DFT) calculations of the [2+2+2] cyclotrimerisation of *p*-X-substituted phenylacetylenes (X = H, NO₂, and NH₂) catalysed by [Rh(BIPHEP)]⁺ were carried out to determine the reaction mechanism in each case and analyse the effect that the electronic character of the substituents has on the regioselectivity. For the rate-determining step corresponding to the oxidative coupling leading to the rhodacyclopentadiene intermediate, we have taken into account two reaction pathways: the reaction pathway with the lowest energy barrier and the reaction pathway through the most stable transition state (Curtin-Hammett pathway). Our results show that the theoretical results conform experimental outcomes for different *p*-X-substituted phenylacetylenes (X = NO₂, F, H, Me, ^tBu, OMe, NMe₂) only when the Curtin-Hammett reaction pathway is considered. A fairly good correlation has been obtained between the electronic nature of the substituents (as expressed by the Hammett σ_{para} constant values) and the regioisomeric ratios experimentally obtained and computationally predicted.

INTRODUCTION

Polysubstituted benzenes are extremely useful compounds that are widely used both in industry and in academia. Since Reppe et al. discovered in 1948 that nickel catalysed the [2+2+2] cyclotrimerisation of three alkynes,¹ this process has evolved into an elegant preparative route to polysubstituted benzenes.²

A simplified picture of the most generally accepted mechanism of the [2+2+2] cyclotrimerisation, supported by experimental evidences³ and computational studies,⁴⁻⁷ is shown in Scheme 1. The reaction begins via a pair of ligand-alkyne substitution reactions. The oxidative coupling of the two alkyne ligands then generates a metallacyclopentadiene **IIIa** or a metallacyclopentatriene **IIIb** with a biscarbene structure. Subsequent coordination of a third alkyne ligand to **IIIa** or **IIIb** intermediates is followed by either alkyne insertion to form a metallacycloheptatriene **V** (the so-called Schore's mechanism)⁸ or metal-mediated [4+2] cycloaddition to yield the metallanorbornadiene **VI** or [2+2] cycloaddition to give a metallabicyclo[3.2.0]heptatriene **VII**. Finally, the arene **VIII** is formed by reductive elimination of the metal.

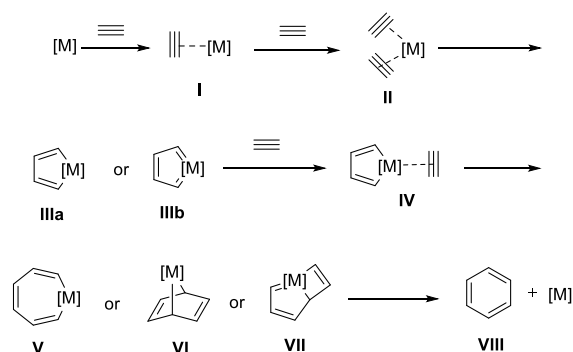
A successful control of the regioselectivity in the intramolecular version of the [2+2+2] cycloaddition reactions is

generally accomplished by altering the positions of the alkynes in the linear substrate and/or by modulating the strain in the intermediates or products. On the other hand, successful regiocontrol in a fully intermolecular reaction is much more challenging.⁹ In the intermolecular [2+2+2] cyclotrimerisation of three identical monosubstituted alkynes, there is no chemoselectivity but regioselectivity remains a problem. Scheme 2 shows the two possible regioisomers, 1,2,4-trisubstituted benzene and 1,3,5-trisubstituted benzene, that can be formed in the cycloaddition process.

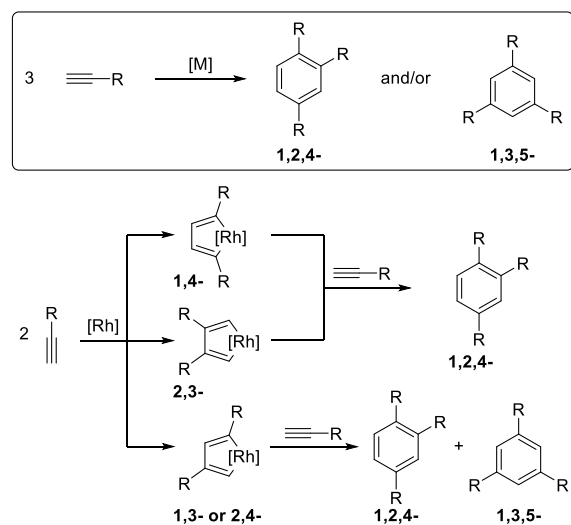
The formation of the two regioisomers of Scheme 2 can be understood following the postulated general mechanism for this reaction. In the case of the rhodium(I)-catalysed cyclotrimerisation reactions, in the formation of the rhodacyclopentadiene **III**, the two alkynes can be coupled oxidatively to the rhodium(I) in three or four (depending on the symmetry of the catalyst) different ways, namely, head-to-head, tail-to-tail, tail-to-head, and head-to-tail giving the 1,4, 2,3, and 1,3/2,4 regioisomeric metallacyclopentadienes (Scheme 2). In this notation, we consider the phenyl group as the tail of the phenylacetylene molecule. In the subsequent insertion of the third alkyne and posterior reductive elimination, intermediates 1,4 and 2,3 only afford regioisomer 1,2,4-, and only intermediates 1,3/2,4

can give regioisomers 1,2,4- or 1,3,5-. As can be seen in Scheme 2, it is more likely to form regioisomer 1,2,4- than regioisomer 1,3,5-, if we suppose similar energy barriers for the formation of all intermediates. It can be concluded that there are two crucial steps in obtaining high selectivity in the formation of one of the regioisomers: i) the selective formation of metallacyclopentadiene intermediate and ii) in the case of intermediate 1,3/2,4 the regioselective insertion of the third alkyne. This second aspect is crucial for the formation of the 1,3,5-regioisomer.

Scheme 1. Generally accepted mechanism for the [2+2+2] cyclotrimerisation reaction of three alkynes. [M] = transition metal.



Scheme 2. Possible regioisomers in the [2+2+2] cyclotrimerisation of three identical terminal alkynes and their mechanism of formation.



Substantial research efforts have been devoted to the development of reaction conditions and catalytic systems that allow the regioselective synthesis of polysubstituted benzenes.¹⁰ The regioselectivity ratios obtained have been rationalised mainly based on steric grounds but also on the basis of electronic effects in some examples,¹¹ but there is

not a clear consensus on how the steric and electronic effects govern the process, so there is a lack for predictive criteria.

To gain insight into the factors that govern the regioselectivity in the [2+2+2] cycloaddition reactions we decided to study the cyclotrimerisation of differently *p*-X-substituted phenylacetylenes both experimentally and by means of density functional theory (DFT) calculations. We selected the cases X = H, NO₂, and NR₂ (R = H in the computational study and R = CH₃ in experiments) with the aim to discuss electronic effects in this cyclotrimerisation. Rhodium has been chosen as transition-metal in the catalytic system since is one of the most often used catalyst. In particular, we considered the cationic [Rh(BIPHEP)]⁺ catalyst, (BIPHEP=2,2-bis(diphenylphosphino)-1,1-biphenyl), as it has been widely used for these [2+2+2] cycloaddition reactions.²

RESULTS AND DISCUSSION

Let us start the discussion by analyzing the [2+2+2] cyclotrimerisation of unsubstituted phenylacetylene to yield 1,2,4- and 1,3,5-triphenylbenzene. The phenyl group has a weak π -donor and inductive withdrawing character¹² that makes phenylacetylene a mild electron deficient alkyne.¹³ The Gibbs energy profile obtained for the [2+2+2] cyclotrimerisation of phenylacetylene catalysed by [Rh(BIPHEP)]⁺ is shown in Scheme 3. There is a preactivation scenario that transforms **A0** to **A2** in an exergonic process by ca. 40 to 50 kcal/mol. On the other hand, the catalytic cycle that involves **A2** species is very exergonic by about 130 to 145 kcal/mol. This huge thermodynamic driving force is generated by the formation of three new C-C σ bonds and the gain of aromatic stabilisation energy. Somewhat unexpectedly, 1,3,5-triphenylbenzene is 1.6 kcal/mol less stable than 1,2,4-triphenylbenzene. π - π stacking interactions between adjacent phenyl groups in 1,2,4-triphenylbenzene makes this compound more stable than its 1,3,5-regioisomer. Formation of 1,3,5-triphenylbenzene is, therefore, statistically (only 25% of the possible reaction paths leads to its formation, Scheme 2) and thermodynamically disfavoured.

To discuss the kinetic preferences of the two isomers, we have to analyse the entire reaction mechanism. In the first step, the interaction of one phenylacetylene with the [Rh(BIPHEP)]⁺ catalyst yields 14-electron intermediate **A1** and stabilizes the system by 31.3 kcal/mol. In the second step, a second phenylacetylene molecule coordinates to the metal center to form **A2**. This interaction can occur in four different ways, namely, tail-to-tail (**A2**_{2,3}), head-to-head (**A2**_{1,4}), tail-to-head (**A2**_{1,3}), and head-to-tail (**A2**_{2,4}, see Scheme 3). Depending on the orientation of the two phenylacetylenes, the stabilisation energy of **A2** with respect to **A1** and a free phenylacetylene ranges from 10.0 to 19.0 kcal/mol, the most stable **A2** intermediates being the head-to-head **A2**_{1,4} and the head-to-tail **A2**_{2,4} isomers. Unsurprisingly, for steric reasons, the tail-to-tail **A2**_{2,3} disposition of the two ligands leads to the less stable **A2** intermediate. On the other hand, the tail-to-head

A2_{1,3} isomer is 6.1 kcal/mol less stable than the head-to-tail **A2**_{2,4} intermediate because in the former there is some steric repulsion between one of the phenyl groups of the BIPHEP ligand and the triple bond of one phenylacetylene (distance H_{BIPHEP}-C_{phenylacetylene} of 2.533 Å). It is likely that the different **A2** species may reach equilibrium. Given the transformation between **A2** species, which require turning back to **A1**, is feasible, Curtin-Hammett¹⁴ conditions are applicable. For this reason, we have decided to study both the reaction path with the lowest energy barrier and the Curtin-Hammett predicted path.

From **A2**, the system evolves to give the rhodacyclopentadiene **A3** intermediate through an oxidative coupling. From the work by Stockis and Hoffmann,¹⁵ we know that, if steric effects are unimportant, the oxidative coupling places the C atom with electron-withdrawing substituents next to the metal. Thus, from an electronic point of view, the 1,4-coupling should be favoured and the 2,3- should have the largest energy barrier. One can expect the same ordering taking into account steric effects among phenylacetylenes. Indeed, when substituents of terminal alkynes are bulky, the steric factor is the one that controls the selectivity of the oxidative coupling.¹⁶ In our particular case, steric and electronic effects point to the same conclusion for the oxidative coupling of two phenylacetylenes.

Results in Scheme 3 show that, as predicted on the basis of electronic and steric effects, the 2,3-coupling is the one having the less stable transition state (TS) for the oxidative coupling. On the other hand, TSs for the 1,4- and 2,4-coupling have the lowest energies (Scheme 3), but because the **A2** intermediate in the 1,3-coupling is less stable than those of the 1,4- and 2,4-couplings, the oxidative coupling with the lowest energy barrier corresponds to the tail-to-head 1,3-attack (**A2**_{1,3} in green in Scheme 3). The Gibbs energy barrier for this 1,3-oxidative coupling through **TS(A2,A3)** is 17.4 kcal/mol, about 2 kcal/mol less than for any of the other couplings (see Table 1). This is the highest energy barrier throughout the catalytic cycle and, therefore, is the rate determining step (rds) as found in some other [2+2+2] cyclotrimerisations.^{4a,5a,6b,6c,6e,7a,17} Given that for our system, Curtin-Hammett conditions are applicable, the reaction can also evolve from **A3**_{2,4} (in grey in Scheme 3) that has the transition state lowest in energy. Under Curtin-Hammett conditions, the barrier has to be computed with respect to the lowest in energy intermediate, and, therefore, formation of **A3**_{2,4} through **TS(A2,A3)** has an energy barrier of 22.2 kcal/mol. It is important to note that both intermediates, which differ in the relative orientation of the BIPHEP moiety and the rhodacyclopentadiene, can provide either the 1,2,4- or the 1,3,5-triphenylbenzene depending on the insertion step.

The rhodacyclopentadiene ring in **A3**_{1,3} intermediate has a short-long-short C_α-C_β-C_β-C_α sequence (1.347, 1.477, and 1.353 Å), indicating that the π-bonds are quite localised and there is no aromaticity in this five-membered ring.^{6b,7c} The same pattern is observed in all of the rhodacyclopentadiene intermediates studied.

It is worth to compare the Gibbs energy profile of the [2+2+2] cyclotrimerisation catalysed by [Rh(BIPHEP)]⁺ of phenylacetylene with that of acetylene. The latter can be found in the Supporting Information. The energy barrier of the oxidative coupling of two acetylenes is 3.1 kcal/mol lower than that found for the 1,3-oxidative coupling of two phenylacetylenes. This result is somewhat unexpected, since it has been reported that electron-withdrawing groups facilitate the oxidative coupling by lowering the LUMO of the π-bond.^{4b,7c} It is likely that steric effects are responsible for the increase in the energy barrier when going from acetylene to phenylacetylene.

Coming back to the [2+2+2] cyclotrimerisation of phenylacetylene catalysed by [Rh(BIPHEP)]⁺, let us discuss first the evolution of the intermediate coming from the lowest barrier in the oxidative coupling. Once the 1,3-diphenylrhodacyclopentadiene **A3**_{1,3} is formed, another phenylacetylene molecule coordinates to Rh to yield the 16-electron intermediate **A4** and releasing about 18 kcal/mol. The molecular structure of the resulting complex is similar to the only reported example of a metallacyclopentadiene(alkyne) species.¹⁸ Interestingly, in this case, the addition of the new coordinated phenylacetylene molecule to the 1,3-diphenylrhodacyclopentadiene occurs through an insertion on to the Rh-C bond (Schore's mechanism). We tried to locate the rhodanorbornadiene and rhodabicyclo[3.2.0]heptatriene intermediates but all our attempts failed, and, consequently, presence of these intermediates in the reaction mechanism was ruled out. The insertion through the Schore's mechanism does not generate the expected rhodacycloheptatriene or the four- and five-membered bicyclic intermediate. Instead of that, the reaction evolves directly to the formation of **A5**, i.e., the product η⁶-coordinated to the Rh[BIPHEP]⁺ with Rh-C_{benzene} distances ranging from 2.26 to 2.47 Å. For the insertion process, we have analysed all four possible insertions of the phenylacetylene molecule to the rhodacyclopentadiene complex (Scheme 4, first row). The two attacks in which the phenylacetylene is inserted into the Rh-C_α bond of the rhodacyclopentadiene complex with the C_α being attached to a hydrogen (types I and II) were found to lead to **A5** intermediate with low Gibbs energy barriers. The insertions onto the Rh-C_α bond in which the C_α is attached to the phenyl (types III and IV) were found to have barriers higher by at least 9.3 kcal/mol. Type I insertions are usually preferred for electrostatic reasons. The unsubstituted C atoms in phenylacetylene and rhodacyclopentadiene are more negatively charged than the C atoms with Ph substituents having electron withdrawing character. Based on electrostatic grounds,¹⁹ the more negatively charged unsubstituted C atom in phenylacetylene interacts better with the metal and the less negatively charged C atom in phenylacetylene prefers the unsubstituted C_α of the rhodacyclopentadiene.

Scheme 3. Gibbs energy profile (in kcal/mol) for the [2+2+2] cycloaddition reaction of three phenylacetylenes catalysed by [Rh(BIPHEP)]⁺. Four possible oxidative coupling pathways have been explored but from **A3** only two paths have been followed, the lowest energy barrier path (in green) leading to the 1,3,5 isomer and the Curtin-Hammett favoured path (in grey) leading to the 1,2,4 isomer.

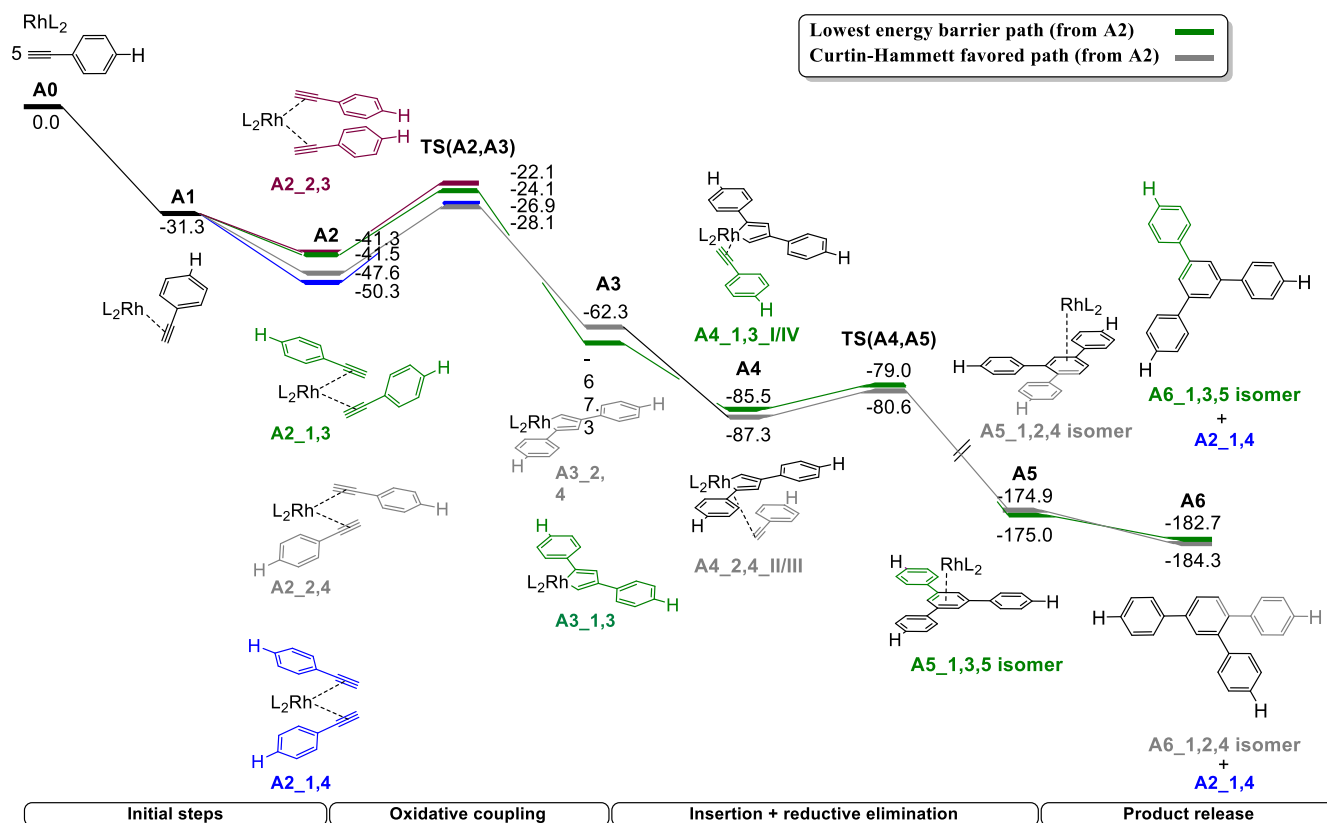


Table 1. Gibbs energy barriers (in kcal/mol) for the oxidative coupling step in the [2+2+2] cyclotrimerisation reaction of *p*-X-substituted phenylacetylenes catalysed by Rh[BIPHEP]⁺ (TS(A₂,A₃)).

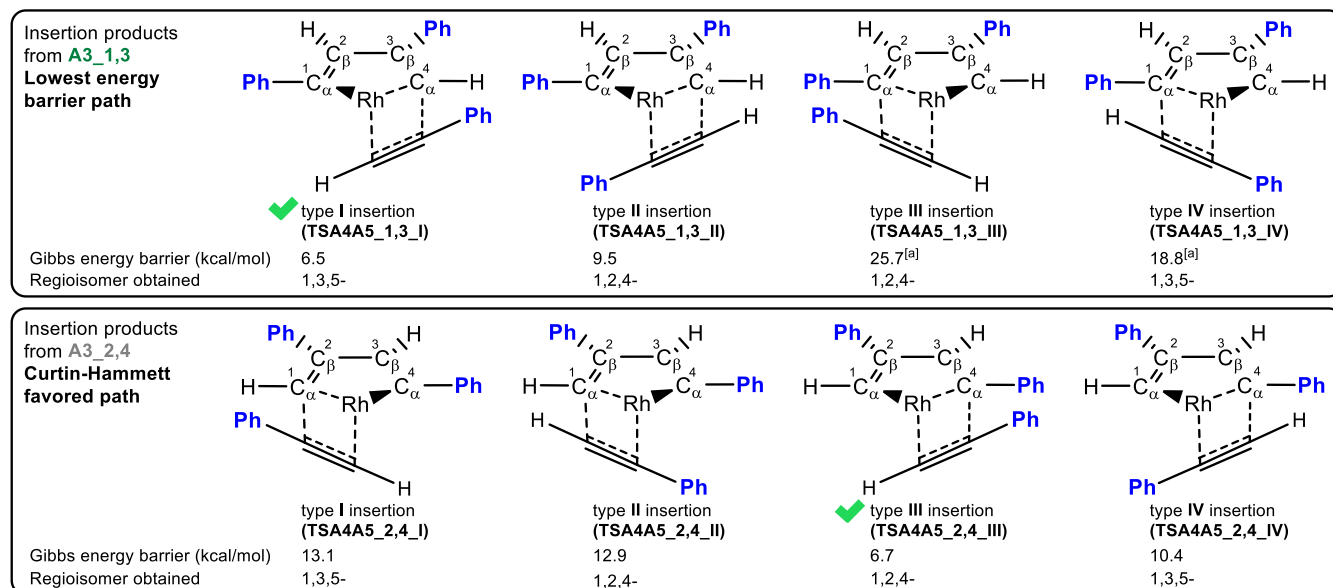
Coupling	X = H	X = NO ₂	X = NH ₂	Regioisomer
1,4	23.4	16.6	18.8	1,2,4-
2,4	19.5	17.4	16.8	1,2,4- OR 1,3,5-
2,3	19.2	21.5	18.5	1,2,4-
1,3	17.4	21.9	13.9	1,2,4- OR 1,3,5-

As for the oxidative coupling process, in the insertion step, we also considered the possibility that the different metallacyclopentadiene(alkyne) complexes **A4** were in equilibrium. However, the barriers for the insertion are lower than those for the conversion of **A4** into **A3**, so the Curtin-Hammett conditions are not fulfilled in this insertion process.

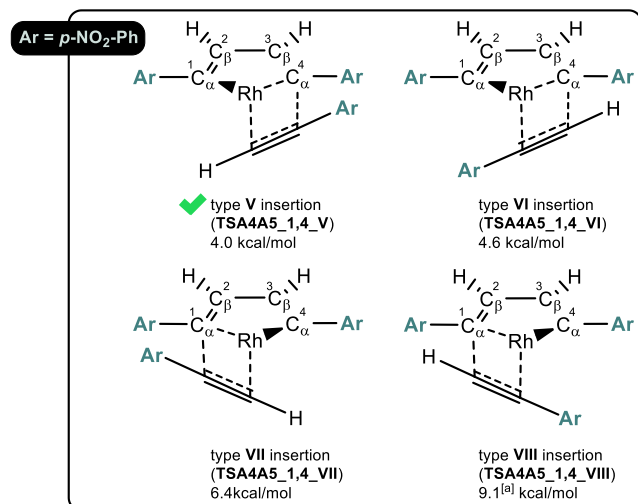
Now, let us move to the evolution of the intermediate **A3**_{2,4}, that comes from the Curtin-Hammett path in the oxidative coupling reaction (in grey in Scheme 3). We have again analysed all four possible insertions of the phenylacetylene molecule to the rhodacyclopentadiene complex (Scheme 4, second row). In this case, the insertion with the lowest barrier (6.7 kcal/mol) takes place onto the Rh-C_α bond in which the C_α is attached to the phenyl (type III) and leads to the 1,2,4-regioisomer. The preference for this insertion as compared to type I seems to arise from a better π-π interaction in the transition state of the type III insertion. A type IV insertion from **A3**_{2,4} yields the 1,3,5-regioisomer with a barrier of 10.4 kcal/mol. Using the transition state theory, one predicts a 99:1 (1,2,4-:1,3,5-) ratio of regioisomers.

As a whole, whereas the path with the lowest energy barrier for the oxidative coupling generates preferentially the 1,3,5-triphenylbenzene (with a predicted 1:99 1,2,4-:1,3,5-regioisomeric ratio using the transition state theory), the pathway that is followed under Curtin-Hammett conditions leads preferentially to the 1,2,4-triphenylbenzene (99:1 ratio). If the two pathways were operative and equally favoured, we would predict the formation of a ca. 50:50

Scheme 4. Gibbs energy barriers (in kcal/mol) for the insertion of phenylacetylene in the 1,3- or 2,4-diphenylrhodacyclopentadiene (**TS(A₄,A₅)**). A green tick indicates the preferred pathway (insertion with the lowest barrier).^[a] Despite many attempts to fully optimize the TS for this approach, this TS was optimised only for the forces but not for the displacements due to very flat potential energy surface. Therefore, the reported Gibbs energy barrier represents an estimation that we think should be close to the exact value.



Scheme 5. Gibbs energy barriers (in kcal/mol) for the insertion of *p*-NO₂-phenylacetylene in the 1,4-dinitrophenylrhodacyclopentadiene (**TS(A₄,A₅)**). A green tick indicates the preferred pathway (insertion with the lowest barrier).^[a] Despite many attempts to fully optimize the TS for this approach, this TS was optimised only for the forces but not for the displacements due to very flat potential energy surface. Therefore, the reported Gibbs energy barrier represents an estimation that we think should be close to the exact value.



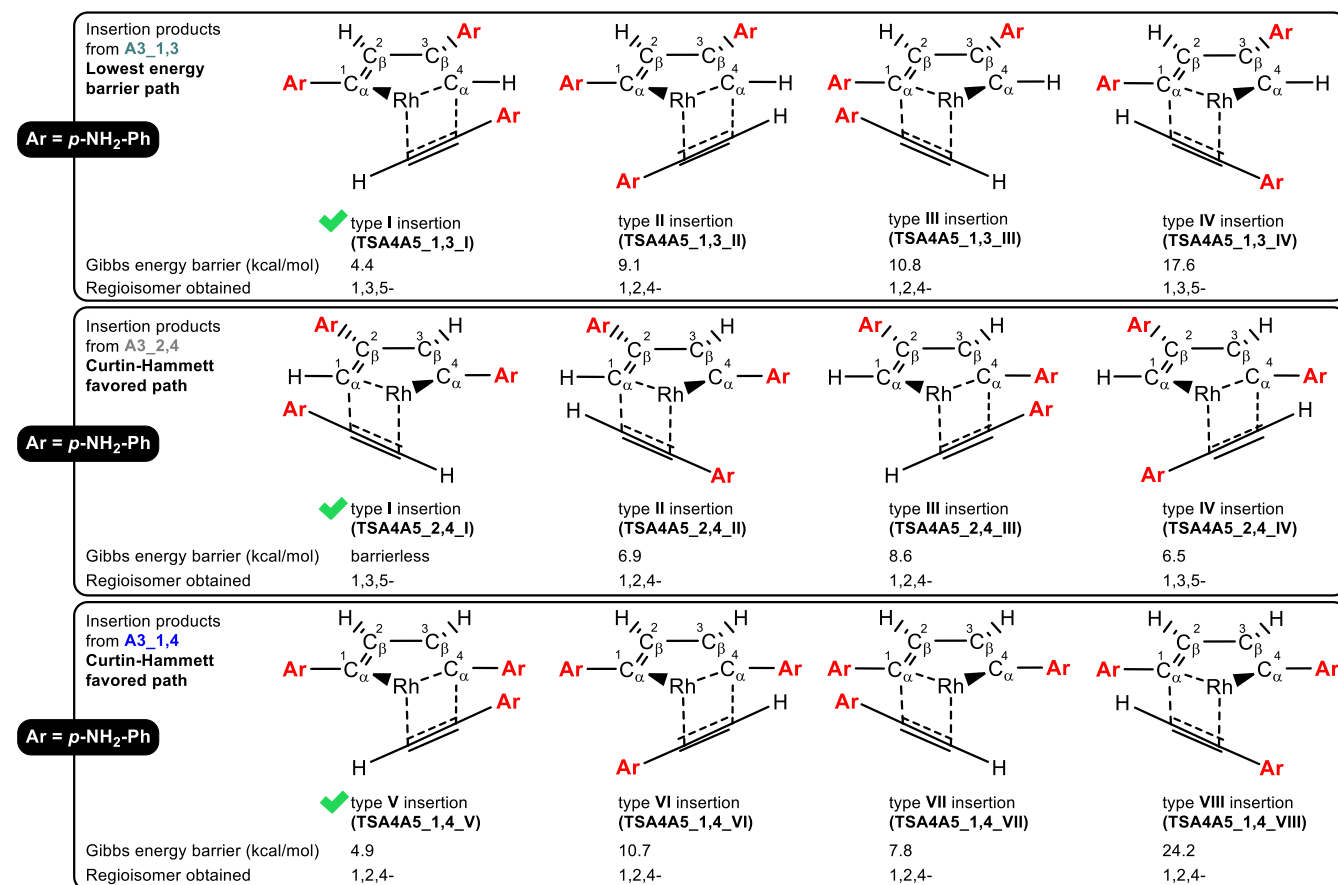
mixture of 1,2,4- and 1,3,5-triphenylbenzene as a result of competing paths of similar energy barriers. However, experimental (theoretical) results found a 96:4 (99:1) ratio of

the two regioisomers (*vide infra*), the 1,2,4-triphenylbenzene being clearly favoured. This result indicates that the Curtin-Hammett pathway is the preferred one in the Rh-catalysed alkyne cyclotrimerisation.

Final release of the product from **A₅** is assisted by the addition of two phenylacetylene molecules directly regenerating intermediate **A₂**.

Next, we increased the electron-withdrawing character of the phenyl group by adding a nitro substituent in the *para* position of phenyl group, i.e., we studied the cyclotrimerisation of *p*-nitrophenylacetylene catalysed by [Rh(BIPHEP)]⁺. The Gibbs energy profile for this [2+2+2] cyclotrimerisation is given in the Supporting Information (Scheme S1). Electron-withdrawing effects of *p*-nitrophenyl group are now enhanced and, as a result, the barrier for the 2,3-attack increases and that of the 1,4-oxidative coupling decreases (Table 1). Therefore, this 1,4-transition state is now the most stable and also it is the oxidative coupling with the lowest energy barrier. Consequently, calculations predict the formation of *only the 1,2,4-regioisomer*. For the 1,4-di-*p*-nitrophenylrhodacyclopentadiene, the type V insertion (Scheme 5) has the lowest energy barrier (4.0 kcal/mol) and the lowest in energy transition state. We name type V to VIII insertions because, at variance with insertions in 1,3- and 2,4-diphenylrhodacyclopentadienes, in 1,4-diphenylrhodacyclopentadienes, the two possible Rh-C_α insertions have C_α atoms with Ph substituents. The insertion reaction is more favourable for the *p*-nitrophenylacetylene molecules than for the phenylacetylenes. The insertion leads to intermediate **A₅** (the product η⁶ coordinated to [Rh(BIPHEP)]⁺) that subsequently releases

Scheme 6. Gibbs energy barriers (in kcal/mol) for the insertion of *p*-aminophenylacetylene in the 1,3-, 2,4- or 1,4-diaminophenylrhodacyclopentadiene (**TS(A4,A5)**). A green tick indicates the preferred pathway (insertion with the lowest barrier).



the 1,2,4-tri-*p*-nitrophenylbenzene in the final reductive elimination process. As a whole, the route followed in the [2+2+2] cyclotrimerisation of *p*-nitrophenylacetylene is the one corresponding to the 1,4-oxidative coupling always leading exclusively to the 1,2,4-tri-*p*-nitrophenylbenzene.

Finally, we reduced the electron-withdrawing character of the phenyl group by adding an amino substituent in the *para* position of phenyl group, i.e., we studied the cycloaddition of *p*-aminophenylacetylene catalysed by [Rh(BIPHEP)]⁺. The Gibbs energy profile for this [2+2+2] cyclotrimerisation is given in the Supporting Information (Scheme S2). Electron-donating effects of the amino group result in a decrease of the barrier for the 2,3-attack and in an increase of the 1,4-oxidative coupling when compared to those of the *p*-nitrophenylacetylene (Table 1). For steric reasons, the tail-to-head (**A2_1,3**) disposition of the two ligands leads to the less stable **A2** intermediate. This intermediate is connected to the **TS(A2,A3)** of the 1,3-oxidative coupling that has the lowest Gibbs energy barrier (13.9 kcal/mol). The Gibbs energy barriers of the rest of possible oxidative couplings are, at least, 2.9 kcal/mol higher in energy. We also considered the pathways that start with the

head-to-head (**A2_1,4**) and head-to-tail (**A2_2,4**) dispositions of the two *p*-aminophenylacetylenes that correspond to the transition states lowest in energy (Curtin-Hammett pathways). These two transition states differ by only 0.1 kcal/mol, and for this reason we analysed two Curtin-Hammett paths for this cyclotrimerisation. This 0.1 kcal/mol energy difference corresponds to a product ratio of 54:46 in favour of the 1,2,4-regioisomer (considering that **A2_1,4** leads to 1,2,4-regioisomer and that **A2_2,4** evolves to 1,3,5-regioisomer, *vide infra*). Once the 1,3-, 1,4-, or 2,4-di-*p*-aminophenylrhodacyclopentadiene intermediate **A3** is formed, another *p*-aminophenylacetylene molecule coordinates to Rh to yield the 16-electron intermediate **A4** and releasing about 20 kcal/mol depending on the orientation of the incoming molecule. As for the path through the lowest energy barrier for the phenylacetylene, type I insertions onto 1,3- and 2,4-di-*p*-aminophenylrhodacyclopentadiene intermediates, in which the *p*-aminophenylacetylene is inserted into the Rh-C_α bond of the rhodacyclopentadiene complex with the unsubstituted C_α were found to lead to **A5** intermediate with low Gibbs energy barriers (Scheme 6). For 1,4-di-*p*-aminophenylrhodacyclopentadiene, type V

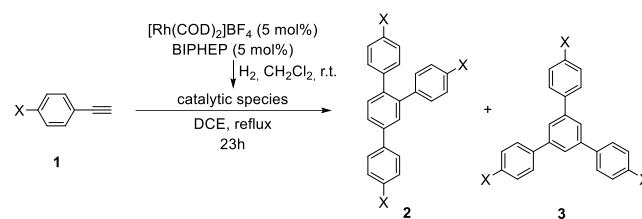
insertion is preferred, as in the case of *p*-nitrophenylacetylene. The Gibbs energy barrier for the transformation of **A4** into **A5** are 4.4 kcal/mol for the type I insertion in **A4_1,3** leading to the 1,3,5-isomer, 4.9 for the type V insertion in **A4_1,4** producing the 1,2,4-isomer, whereas the type I insertion in **A4_2,4** is barrierless and yields the 1,3,5-regioisomer (see Schemes 6 and S2). In all cases, these paths represent the insertion with both the lowest transition state and the lowest energy barrier. Although, formation of the 1,3,5-isomer is slightly favoured thermodynamically (by 1.5 kcal/mol), from a kinetic point of view and given the existence of multiple paths with relatively low Gibbs energy barriers, it is likely that, experimentally, a mixture of 1,3,5- and 1,2,4-tri-*p*-aminophenylacetylenebenzene will be formed. In particular, the Curtin-Hammett pathway, which is found to be the preferred one in the Rh-catalysed alkyne cyclotrimerisation of phenylacetylene, produces a mixture of the 1,2,4-isomer coming from the **A4_1,4** intermediate via type V insertion and the 1,3,5-regioisomer generated from type I insertion in **A4_2,4**.

To check experimentally the conclusions from the theoretical results, we conducted the rhodium-catalysed [2+2+2] cyclotrimerisation of a series of commercially available *p*-substituted phenylacetylenes **1** (Table 2) with different electronic demand (X = H, X = NO₂ and X = NH₂ that has been replaced by X = NMe₂) including the substrates studied theoretically.²⁰ A combination of cationic rhodium complex [Rh(COD)₂]BF₄ and BIPHEP as the biphosphine was selected as the catalytic system. Using a 5 mol% of the catalytic system [Rh(COD)₂]BF₄/BIPHEP in dichloroethane as the solvent, the reaction was carried out under reflux. The results obtained are shown in Table 2 together with the Hammett substituent σ_{para} constants of the different substrates.²¹ Every reaction was run twice in the same reaction conditions to check the reproducibility of the method, especially in the case of the ratio between regioisomers. The low yields of the NO₂, F and NMe₂ cases is due to the polymerization of the *para*-substituted phenylacetylenes and formation of decomposition products.

The correlation between the ratio of 1,2,4(**2**):1,3,5(**3**) regioisomers formed and the Hammett substituent σ_{para} constants is fairly good. The highly electronwithdrawing nitro group yielded the 1,2,4-regioisomer **2** exclusively and no traces of the 1,3,5-regioisomer **3** were detected (entry 1, Table 2), as was predicted with our DFT calculations. On the other extreme, when the reaction was run with *p*-dimethylaminophenylacetylene (entry 7, Table 2), the cyclotrimerisation gave a mixture of the two regioisomers in a 59:41 ratio (as compared to theoretical 54:46 prediction). When *p*-aminophenylacetylene was calculated, two possible insertions (**A3_2,4** and **A3_1,4**) were possible, each one leading to the formation of one different isomer, and so a mixture of both isomers could be expected which is what is observed experimentally. The remaining substrates, comprising substituents with σ_{para} values ranging from 0.06 to -0.27 (entries 2-6, Table 2) led to regioisomeric mixtures ranging

from 96:04 to 81:19, highly enriched with the 1,2,4- regioisomer. In the cyclotrimerisation of phenylacetylene following the Curtin-Hammett calculated path, the type III insertion from **A3_2,4** is the most favoured explaining why the 1,2,4 isomer was the one obtained predominantly in the experiments, a result which we think can be extrapolated to all this set of substituents.

Table 2. [Rh(COD)₂]BF₄ / BIPHEP-catalysed [2+2+2] cyclotrimerisation of phenylacetylene derivatives **1**.^a



Entry	X	σ_{para}	Yield ^b (%) (2+3)	Ratio ^c (2:3)
1	NO ₂	0.78	38	100:0
2	F	0.06	36	92:08
3	H	0	62	96:04
4	Me	-0.17	96	95:05
5	^t Bu	-0.20	92	81:19
6	OMe	-0.27	65	94:06
7	NMe ₂	-0.83	33	59:41

^a Reaction conditions: [Rh(COD)₂]BF₄ (0.025 mmol), BIPHEP (0.025 mmol), alkyne (0.5 mmol), DCE (3 mL) at reflux for 3 hours (X = H and NO₂) or reflux for 23 hours (X = F, Me, ^tBu, OMe, NMe₂). ^b Isolated yield. ^c Ratio was determined by ¹H NMR of the crude mixture except in the case of *p*-fluorophenylacetylene in which ¹⁹F NMR was used.

CONCLUSIONS

We performed density functional theory (DFT) calculations of three *p*-X-substituted phenylacetylenes (X = H, NO₂, and NH₂) and experimental studies of seven *p*-X-substituted phenylacetylenes (X = NO₂, F, H, Me, ^tBu, OMe, NMe₂) in the [2+2+2] cyclotrimerisation catalysed by [Rh(BIPHEP)]⁺ to analyse the effect of the electronic character of the substituents on the regioselectivity of the reaction. Our theoretical and experimental results show that *p*-nitrophenylacetylene, which have the most electron withdrawing substituent, yields exclusively the 1,2,4-regioisomer by favouring the head-to-head oxidative coupling. On the other hand, when X = H, the 1,2,4-regioisomer is formed preferentially, whereas when X = NMe₂ a 59:41 mixture of both isomers is obtained. These experimental results provide evidence that, from the two possible reactions pathways analysed computationally (lowest in energy barrier and Curtin-Hammett paths), the Curtin-Hammett

pathway is the operative one and, therefore, is the one governing the regioselectivity.

EXPERIMENTAL SECTION

Representative methods

Unless otherwise noted, materials were obtained from commercial suppliers and used without further purification. Reactions requiring anhydrous conditions were conducted in oven-dried glassware under a dry nitrogen atmosphere. Dichloromethane was degassed and dried under a nitrogen atmosphere by passing through solvent purification columns (MBraun, SPS-800). Solvents were removed under reduced pressure with a rotary evaporator. Reaction mixtures were chromatographed on a silica gel column (230-400 mesh) by using a gradient solvent system as the eluent.

General procedure for [2+2+2] cycloaddition reactions of *p*-substituted phenylacetylenes: In a 10 mL flask, a mixture of [Rh(COD)₂]BF₄ (0.025 mmol) and BIPHEP (0.025 mmol) was dissolved in CH₂Cl₂ (3 mL). Hydrogen gas was introduced to the catalyst solution and stirred for 30 min. The resulting mixture was then concentrated to dryness. Dichloroethane (2 mL) was added and the solution was stirred under a N₂ atmosphere and heated at 80 °C. A solution of phenylacetylene **1** (0.5 mmol) in dichloroethane (1 mL) was then added to the pre-heated catalytic mixture. The reaction mixture was then stirred at reflux until completion (TLC and GC monitoring). The solvent was evaporated and the residue was purified by column chromatography on silica gel.

Computational details

Geometries of the reactants, intermediates, transition states (TSs), and products were optimised using the DFT B₃LYP²² hybrid exchange-correlation functional with the Gaussian09²³ program. All geometry optimisations were performed without symmetry constraints. In all calculations the D₃ Grimme energy correction for dispersion²⁴ with the Becke-Johnson damping function²⁵ were included. The all-electron cc-pVDZ basis set²⁶ was employed for non-metal atoms and the cc-pVDZ-PP basis set containing an effective core relativistic pseudopotential was used for Rh.²⁷ The same method (B₃LYP-D₃) with a similar double- ξ basis set with polarised functions has been recently recommended to predict product concentrations.²⁸ Results reported are limited to the singlet state potential energy surfaces. However, we calculated the triplet state for all reactants, intermediates, transition states, and products and we found that triplet states were higher in energy in all cases and, therefore, were not considered in the reaction path. The electronic energy was improved by performing single point calculations with the aug-cc-pVTZ (cc-pVTZ-PP for Rh) basis set. Analytical Hessians were computed to determine the nature of stationary points (one and zero imaginary frequencies for TSs and minima, respectively) and to calculate unscaled zero-point energies (ZPEs) as well as thermal corrections and entropy effects using the standard statistical-mechanics relationships for an ideal gas.²⁹ These two latter terms were computed at 353.15 K (temperature of experiments) and 1 atm to provide the reported relative Gibbs energies (ΔG). Entropy corrections were divided by a factor of 2 to correct for the overestimation suffered by gas-phase entropies when used to determine entropies for reactions in solution.³⁰ Finally, solvation Gibbs energies in dichloroethane were calculated with the B₃LYP-D₃/cc-pVDZ-PP method using the PCM continuum solvation model³¹ at the gas-phase geometries. The resulting solvation Gibbs energies were added to the final Gibbs energies in gas-phase to obtain Gibbs energies in solution. Standard

Gibbs energies in solution refer to a 1 M standard-state concentration for all species. The change of conventional 1 atm standard state for gas-phase calculations to a standard-state gas-phase concentration of 1 M requires the introduction of a concentration change energy term of 2.36 kcal/mol at 353.15 K.³² As a summary, the hereafter reported Gibbs energies contain electronic energies calculated at the B₃LYP-D₃/aug-cc-pVTZ-PP//B₃LYP-D₃/cc-pVDZ-PP level together with gas phase thermal corrections and entropic contributions (the latter divided by two) at 353.15 K as well as the 2.36 kcal/mol term of changing the standard states from 1 atm to 1 M and the solvation energies computed with the B₃LYP-D₃/cc-pVDZ-PP method. Furthermore, the connectivity between stationary points was unambiguously established by intrinsic reaction path³³ calculations. The Cartesian coordinates of all minima and TSs located can be found in the Supporting information.

ASSOCIATED CONTENT

Supporting Information

Characterization data for the cyclotrimerized products, Gibbs energy profiles (in kcal/mol) for the [2+2+2] cyclotrimerisation reaction catalysed by Rh[BIPHEP]⁺ of three 4-nitrophenylacetylenes, three 4-aminophenylacetylenes, and three acetylenes (pdf file) together with Cartesian coordinates of all minima and transition states (text file). The Supporting Information is available free of charge on the ACS Publications website.

AUTHOR INFORMATION

Corresponding Authors

*E-mail: anna.plaq@udg.edu, miquel.sola@udg.edu.

Notes

The authors declare no competing financial interest.

ACKNOWLEDGMENT

Financial support from the Spanish Ministry of Economy and Competitiveness (MINECO) (Project No. CTQ2017-85341-P) and the DIUE of the Generalitat de Catalunya (Project No. 2017SGR39 and ICREA Academia 2014 to M. S.) are acknowledged. Thanks are due to the Generalitat de Catalunya for FI predoctoral grants to Ò.T., M.F. and À.D.-J. The EU under the FEDER grant UNG110-4E-801 has also funded this research.

REFERENCES

- 1) Reppe, W.; Schweckendiek, W.J. Cyclisierende polymerisation von acetylen. III benzol, benzolderivate und hydroaromatische verbindungen. *Justus Liebigs Ann. Chem.* **1948**, *560*, 104-116.
- 2) For selected references, see: a) Saito, S.; Yamamoto, Y. Recent advances in the transition-metal-catalyzed regioselective approaches to polysubstituted benzene derivatives. *Chem. Rev.* **2000**, *100*, 2901-2915; b) Kotha, S.; Brahmachary, E.; Lahiri, K. Transition metal catalyzed [2+2+2] cycloaddition and application in organic synthesis. *Eur. J. Org. Chem.* **2005**, 4741-4767; c) Yamamoto, Y. Recent advances in intramolecular alkyne cyclotrimerization and its applications. *Curr. Org. Chem.* **2005**, *9*, 503-519; d) Gandon, V.; Aubert, C.; Malacria, M. Recent progress in cobalt-mediated [2+2+2] cycloaddition

- reactions. *Chem. Commun.* **2006**, 2209–2217; e) Chopade, P.R.; Louie, J. [2+2+2] Cycloaddition reactions catalyzed by transition metal complexes. *Adv. Synth. Catal.* **2006**, *348*, 2307–2327; f) Agenet, N.; Buisine, O.; Slowinski, F.; Gandon, V.; Aubert, C.; Malacria, M. Cotrimerizations of acetylenic compounds. *Org. React.* **2007**, *68*, 1–291; g) Tanaka, K. Cationic rhodium(I)/BINAP-type bisphosphine complexes: versatile new catalysts for highly chemo-, regio-, and enantioselective [2+2+2] cycloadditions. *Synlett* **2007**, 1977–1993; h) Shibata, T.; Tsuchikama, K. Recent advances in enantioselective [2+2+2] cycloaddition. *Org. Biomol. Chem.* **2008**, *6*, 1317–1323; i) Tanaka, K. Transition-metal-catalyzed enantioselective [2+2+2] cycloadditions for the synthesis of axially chiral biaryls. *Chem. Asian J.* **2009**, *4*, 508–518; j) Zhou, L.; Li, S.; Kanno, K.-i.; Takahashi, T. Recent development for formation of aromatic compounds via metallacyclopentadienes as metal-containing heterocycles. *Heterocycles* **2010**, *80*, 725–738; k) Pla-Quintana, A.; Roglans, A. [2+2+2] Cycloaddition reactions of macrocyclic systems catalyzed by transition metals. A review. *Molecules* **2010**, *15*, 9230–9251; l) Inglesby, P.A.; Evans, P.A. Stereoselective transition metal-catalysed higher-order carbocyclisation reactions. *Chem. Soc. Rev.* **2010**, *39*, 2791–2805; m) Hua, R.; Abrenica, M.V.A.; Wang, P. Cycloaddition of alkynes: atom-economic protocols for constructing six-membered cycles. *Curr. Org. Chem.* **2011**, *15*, 712–729; n) Domínguez, G.; Pérez-Castells, J. Recent advances in [2+2+2] cycloaddition reactions. *Chem. Soc. Rev.* **2011**, *40*, 3430–3444; o) Weding, N.; Hapke, M. Preparation and synthetic applications of alkene complexes of group 9 transition metals in [2+2+2] cycloaddition reactions. *Chem. Soc. Rev.* **2011**, *40*, 4525–4538; p) Broere, D.L.J.; Ruijter, E. Recent advances in transition-metal-catalyzed [2+2+2] cyclo(co)trimerization reactions. *Synthesis* **2012**, *44*, 2639–2672; q) *Transition-metal-mediated aromatic ring construction* (Ed.: K. Tanaka), Wiley, Hoboken, 2013; r) Amatore, M.; Aubert, C. Recent advances in stereoselective [2+2+2] cycloadditions. *Eur. J. Org. Chem.* **2015**, 265–286; s) Domínguez, G.; Pérez-Castells, J. Alkenes in [2+2+2] cycloadditions. *Chem. Eur. J.* **2016**, *22*, 6720–6739; t) Lledó, A.; Pla-Quintana, A.; Roglans, A. Allenes, versatile unsaturated motifs in transition-metal-catalysed [2+2+2] cycloaddition reactions. *Chem. Soc. Rev.* **2016**, *45*, 2010–2023; u) Babazadeh, M.; Soleimani-Amiri, S.; Vessally, E.; Hosseinian, A.; Edjlali, L. Transition metal-catalyzed [2+2+2] cycloaddition of nitrogen-linked 1,6-diyne: a straightforward route to fused pyrrolidine systems. *RSC Adv.* **2017**, *7*, 43716–43736; v) Pla-Quintana, A.; Roglans, A. Chiral induction in [2+2+2] cycloaddition reactions. *Asian J. Org. Chem.* **2018**, *7*, 1706–1718.
- (3) For selected references on detection and isolation of intermediates, see: a) Nishiyama, H.; Niwa, E.; Inoue, T.; Ishima, Y.; Aoki, K. Novel metallacycle complexes from bis(oxazolonyl)pyridine–rhodium(I) species and diynes. *Organometallics* **2002**, *21*, 2572–2574; b) Dachs, A.; Torrent, A.; Pla-Quintana, A.; Roglans, A.; Jutand, A. Rates and mechanism of rhodium-catalyzed [2+2+2] cycloaddition of bisalkynes and a monoalkyne. *Organometallics* **2009**, *28*, 6036–6043; c) Dutta, B.; Curchod, B.F.E.; Campomanes, P.; Solari, E.; Scopelliti, R.; Rothlisberger, U.; Severin, K. Reactions of alkynes with [RuCl(cyclopentadienyl)] complexes: the important first steps. *Chem. Eur. J.* **2010**, *16*, 8400–8409; d) Parera, M.; Dachs, A.; Solà, M.; Pla-Quintana, A.; Roglans, A. Direct detection of key intermediates in rhodium(I)-catalyzed [2+2+2] cycloadditions of alkynes by ESI-MS. *Chem. Eur. J.* **2012**, *18*, 13097–13107; e) Bottari, G.; Santos, L.L.; Posadas, C.M.; Campos, J.; Mereiter, K.; Paneque, M. Reaction of [TpRh(C₂H₄)₂] with dimethyl acetylenedicarboxylate: identification of intermediates of the [2+2+2] alkyne and alkyne–ethylene cyclo(co)trimerizations. *Chem. Eur. J.* **2016**, *22*, 13715–13723.
- (4) For selected references of DFT studies catalysed by Ru, see: a) Kirchner, K.; Calhorda, M.J.; Schmid, R.; Veiros, L.F. Mechanism for the cyclotrimerization of alkynes and related reactions catalyzed by CpRuCl. *J. Am. Chem. Soc.* **2003**, *125*, 11721–11729; b) Yamamoto, Y.; Kinpara, K.; Saigoku, T.; Takagishi, H.; Okuda, S.; Nishiyama, H.; Itoh, K. Cp*RuCl-Catalyzed [2+2+2] cycloadditions of α,ω -diynes with electron-deficient carbon–heteroatom multiple bonds leading to heterocycles. *J. Am. Chem. Soc.* **2005**, *127*, 605–613; c) Dazinger, G.; Torres-Rodrigues, M.; Kirchner, K.; Calhorda, M.J.; Costa, P.J. Formation of pyridine from acetylenes and nitriles catalyzed by RuCpCl, CoCp, and RhCp derivatives—A computational mechanistic study. *J. Organomet. Chem.* **2006**, *691*, 4434–4445; d) Varela, J.A.; Rubín, S.G.; Castedo, L.; Saá, C. “Formal” and standard ruthenium-catalyzed [2+2+2] cycloaddition reaction of 1,6-diyne to alkenes: a mechanistic density functional study. *J. Org. Chem.* **2008**, *73*, 1320–1332; e) Remya, P.R.; Suresh, C.H. Mechanistic studies on acetylene cyclotrimerization catalyzed by Grubbs first and second generation catalysts. *Mol. Catal.* **2017**, *441*, 63–71.
- (5) For selected references of DFT studies catalysed by Co, see: a) Hardesty, J.H.; Koerner, J.B.; Albright, T.A.; Lee, G.-Y. Theoretical study of the acetylene trimerization with CpCo. *J. Am. Chem. Soc.* **1999**, *121*, 6055–6067; b) Dahy, A.A.; Yamada, K.; Koga, N. Theoretical study on the reaction mechanism for the formation of 2-methylpyridine cobalt(I) complex from cobaltacyclopentadiene and acetonitrile. *Organometallics* **2009**, *28*, 3636–3649; c) Agenet, N.; Gandon, V.; Vollhardt, K.P.C.; Malacria, M.; Aubert, C. Cobalt-catalyzed cyclotrimerization of alkynes: the answer to the puzzle of parallel reaction pathways. *J. Am. Chem. Soc.* **2007**, *129*, 8860–8871; d) Dahy, A.A.; Koga, N. Theoretical study of formation of pyridines by interaction of a cobaltacyclopentadiene with model nitriles (hydrogen cyanide or trifluoroacetonitrile): electronic effects of nitriles on the reaction mechanism. *J. Organomet. Chem.* **2010**, *695*, 2240–2250; e) Garcia, P.; Evanno, Y.; George, P.; Sevrin, M.; Ricci, G.; Malacria, M.; Aubert, C.; Gandon, V. Synthesis of aminopyridines and aminopyridones by cobalt-catalyzed [2+2+2] cycloadditions involving yne-ynamides: scope, limitations, and mechanistic insights. *Chem. Eur. J.* **2012**, *18*, 4337–4344; For a revision article comparing Ru and Co, see: f) Varela, J.A.; Saá, C. CpRuCl- and CpCo-catalyzed or mediated cyclotrimerizations of alkynes and [2+2+2] cycloadditions of alkynes to alkenes: a comparative DFT study. *J. Organomet. Chem.* **2009**, *694*, 143–149.
- (6) For selected references of DFT studies catalysed by Rh, see: a) Orian, L.; van Stralen, J.N.P.; Bickelhaupt, F.M. Cyclotrimerization reactions catalyzed by rhodium(I) half-sandwich complexes: a mechanistic density functional study. *Organometallics* **2007**, *26*, 3816–3830; b) Dachs, A.; Torrent, A.; Roglans, A.; Parella, T.; Osuna, S.; Solà, M. Rhodium(I)-catalysed intramolecular [2+2+2] cyclotrimerizations of 15-, 20- and 25-membered azamacrocycles: experimental and theoretical mechanistic studies. *Chem. Eur. J.* **2009**, *15*, 5289–5300; c) Dachs, A.; Osuna, S.; Roglans, A.; Solà, M. Density functional study of the [2+2+2] cyclotrimerization of acetylene catalyzed by Wilkinson’s Catalyst, RhCl(PPh₃)₃. *Organometallics* **2010**, *29*, 562–569; d) Dachs, A.; Roglans, A.; Solà, M. RhCl(PPh₃)₃-Catalyzed intramolecular cycloaddition of

- enediynes: the nature of the tether and substituents controls the reaction mechanism. *Organometallics* **2011**, *30*, 3151–3159; e) Dachs, A.; Pla-Quintana, A.; Parella, T.; Solà, M.; Roglans, A. Intramolecular [2+2+2] cycloaddition reactions of yne-ene-yne and yne-yne-ene enediynes catalysed by Rh(I): experimental and theoretical mechanistic studies. *Chem. Eur. J.* **2011**, *17*, 14493–14507; f) Orian, L.; Swart, M.; Bickelhaupt, F.M. In silico evidence of indenyl effect in acetylene [2+2+2] cyclotrimerization catalyzed by Rh(I) half-metallocenes: reactivity enhancement through metal-slippage. *ChemPhysChem* **2014**, *15*, 219–228; g) Torres, Ò.; Roglans, A.; Pla-Quintana, A.; Luis, J.M.; Solà, M. Computational insight into Wilkinson's complex catalyzed [2+2+2] cycloaddition mechanism leading to pyridine formation. *J. Organomet. Chem.* **2014**, *768*, 15–22; h) Haraburda, E.; Torres, Ò.; Parella, T.; Solà, M.; Pla-Quintana, A. Stereoselective rhodium-catalysed [2+2+2] cycloaddition of linear allene-ene/yne-allene substrates: reactivity and theoretical mechanistic studies. *Chem. Eur. J.* **2014**, *20*, 5034–5045; i) Crandell, D.W.; Mazumder, S.; Evans, P.A.; Baik, M.-H. The origin of the ligand-controlled regioselectivity in Rh-catalyzed [(2+2)+2] carbocyclizations: steric vs. stereoelectronic effects. *Chem. Sci.* **2015**, *6*, 6896–6900; j) Cassù, D.; Parella, T.; Solà, M.; Pla-Quintana, A.; Roglans, A. Rhodium-catalyzed [2+2+2] cycloaddition reactions of linear allene-ene-yne to afford fused tricyclic scaffolds: insights into the mechanism. *Chem. Eur. J.* **2017**, *23*, 14889–14899; k) Artigas, A.; Lledó, A.; Pla-Quintana, A.; Roglans, A.; Solà, M. A computational study of the intermolecular [2+2+2] cycloaddition of acetylene and C₆₀ catalyzed by Wilkinson's catalyst. *Chem. Eur. J.* **2017**, *23*, 15067–15072. l) Artigas, A.; Pla-Quintana, A.; Lledó, A.; Roglans, A.; Solà, M. Expedient preparation of open-cage fullerenes by rhodium(I)-catalyzed [2+2+2] cycloaddition of diynes and C₆₀: an experimental and theoretical study. *Chem. Eur. J.* **2018**, *24*, 10653–10661.
- (7) For selected references of DFT studies catalysed by other metals, see: a) Guo, C.-H.; Wu, H.-S.; Hapke, M.; Jiao, H. Theoretical studies on acetylene cyclotrimerization into benzene catalyzed by CpIr fragment. *J. Organomet. Chem.* **2013**, *748*, 29–35; b) Liu, Z.; Cheng, R.; He, X.; Liu, B. Reactivity and regioselectivity of methylacetylene cyclotrimerization over the Phillips Cr/silica catalyst: a DFT study. *ACS Catal.* **2013**, *3*, 1172–1183; c) Dahy, A.A.; Koga, N. Trimerization of alkynes in the presence of a hydrotris(pyrzoly)borate iridium catalyst and the effect of substituent groups on the reaction mechanism: a computational study. *Organometallics* **2015**, *34*, 4965–4974. d) For a review involving different metals, see: Yamamoto, K.; Nagae, H.; Tsurugi, H.; Mashima, K. Mechanistic understanding of alkyne cyclotrimerization on mono-nuclear and dinuclear scaffolds: [4+2] cycloaddition of the third alkyne onto metallacyclopentadienes and dimetallacyclopentadienes. *Dalton Trans.* **2016**, *45*, 17072–17081.
- (8) Schore, N.E. Transition metal-mediated cycloaddition reactions of alkynes in organic synthesis. *Chem. Rev.* **1988**, *88*, 1081–1119.
- (9) For a highlight, see: a) Galan, B.R.; Rovis, T. Beyond Reppe: building substituted arenes by [2+2+2] cycloadditions of alkynes. *Angew. Chem. Int. Ed.* **2009**, *48*, 2830–2834; *Angew. Chem.* **2009**, *121*, 2870–2874. For selected examples, see: b) Mori, N.; Ikeda, S.-i.; Odashima, K. Chemo- and regioselective cyclotrimerization of monoynes catalyzed by a nickel(0) and zinc(II) phenoxide system. *Chem. Commun.* **2001**, 181–182; c) Ura, Y.; Sato, Y.; Tsujita, H.; Kondo, T.; Imachi, M.; Mitsudo, T.-a. Ruthenium-catalyzed [2+2+2] cycloaddition of three different alkynes. *J. Mol. Catal. A* **2005**, *239*, 166–171; d) Tanaka, K.; Nishida, G.; Ogino, M.; Hirano, M.; Noguchi, K. Enantioselective synthesis of axially chiral biaryls through rhodium-catalyzed complete intermolecular cross-cyclotrimerization of internal alkynes. *Org. Lett.* **2005**, *7*, 3119–3121. For examples using a temporary tether, see: e) Yamamoto, Y.; Ishii, J.-i.; Nishiyama, H.; Itoh, K. Ru(II)-catalyzed chemo- and regioselective cyclotrimerization of three unsymmetrical alkynes through boron temporary tether. one-pot four-component coupling via cyclotrimerization/Suzuki–Miyaura coupling. *J. Am. Chem. Soc.* **2004**, *126*, 3712–3713; f) Yamamoto, Y.; Ishii, J.-i.; Nishiyama, H.; Itoh, K. Cp*⁺RuCl-catalyzed formal intermolecular cyclotrimerization of three unsymmetrical alkynes through a boron temporary tether: regioselective four-component coupling synthesis of phthalides. *J. Am. Chem. Soc.* **2005**, *127*, 9625–9631; g) Heinz, C.; Cramer, N. Synthesis of Fijiolide A via an atropselective paracyclophane formation. *J. Am. Chem. Soc.* **2015**, *137*, 11278–11281; h) Nishigaki, S.; Shibata, Y.; Tanaka, K. Rhodium-catalyzed chemo- and regioselective intermolecular cross-cyclotrimerization of nonactivated terminal and internal alkynes. *J. Org. Chem.* **2017**, *82*, 11117–11125. For examples using alkyne surrogates, see: i) Hara, H.; Hirano, M.; Tanaka, K. Liquid enol ethers and acetates as gaseous alkyne equivalents in Rh-catalyzed chemo- and regioselective formal cross-alkyne cyclotrimerization. *Org. Lett.* **2008**, *10*, 2537–2540.
- (10) For selected references, see: a) Tanaka, K.; Toyoda, K.; Wada, A.; Shirasaka, K.; Hirano, M. Chemo- and regioselective intermolecular cyclotrimerization of terminal alkynes catalyzed by cationic rhodium(I)/modified BINAP complexes: application to one-step synthesis of paracyclophanes. *Chem. Eur. J.* **2005**, *11*, 1145–1156; b) Yoshida, K.; Morimoto, I.; Mitsudo, K.; Tanaka, H. RhCl₃/amine-catalyzed cyclotrimerization of alkynes. *Chem. Lett.* **2007**, *36*, 998–999; c) Kawatsura, M.; Yamamoto, M.; Namioka, J.; Kajita, K.; Hirakawa, T.; Itoh, T. Ruthenium-catalyzed regioselective [2+2+2] cyclotrimerization of trifluoromethyl group substituted internal alkynes. *Org. Lett.* **2011**, *13*, 1001–1003; d) Xi, C.; Sun, Z.; Liu, Y. Cyclotrimerization of terminal alkynes catalyzed by the system of NiCl₂/Zn and (benzimidazolyl)-6-(1-(arylimino)ethyl)pyridines. *Dalton Trans.* **2013**, *42*, 13327–13330.
- (11) a) Takeya, M.; Fujihara, T.; Kasaya, T.; Nagasawa, A. Dinuclear niobium(III) complexes [(NbCl₂(L))₂(μ-Cl)₂(μ-L)] (L = tetrahydrothiophene, dimethyl sulfide): preparation, molecular structures, and the catalytic activity for the regioselective cyclotrimerization of alkynes. *Organometallics* **2006**, *25*, 4131–4137; b) Bu, X.; Zhang, Z.; Zhou, X. Switching from dimerization to cyclotrimerization selectivity by FeCl₃ in the Y[N(TMS)₂]₃-catalyzed transformation of terminal alkynes: a new strategy for controlling the selectivity of organolanthanide-based catalysis. *Organometallics* **2010**, *29*, 3530–3534.
- (12) Hansch, C.; Leo, A.; Taft, R.W. A survey of Hammett substituent constants and resonance and field parameters. *Chem. Rev.* **1991**, *91*, 165–195.
- (13) Batrice, R.J.; McKinven, J.; Arnold, P.L.; Eisen, M.S. Selective oligomerization and [2+2+2] cycloaddition of terminal alkynes from simple actinide precatalysts. *Organometallics* **2015**, *34*, 4039–4050.
- (14) Seeman, J.I. Effect of conformational change on reactivity in organic chemistry. Evaluations, applications, and extensions of Curtin-Hammett Winstein-Holness kinetics. *Chem. Rev.* **1983**, *83*, 83–134.
- (15) Stockis, A.; Hoffmann, R. Metallacyclopentanes and bisolefin complexes. *J. Am. Chem. Soc.* **1980**, *102*, 2952–2962.

- (16) Wakatsuki, Y.; Nomura, O.; Kitaura, K.; Morokuma, K.; Yamazaki, H. Cobalt metallacycles. II. On the transformation of bis(acetylene)cobalt to cobaltacyclopentadiene. *J. Am. Chem. Soc.* **1983**, *105*, 1907-1912.
- (17) Dalla Tiezza, M.; Bickelhaupt, F.M.; Orian, L. Group 9 metallacyclopentadienes as key intermediates in [2+2+2] alkyne cyclotrimerizations. Insight from activation strain analyses. *ChemPhysChem* **2018**, *19*, 1766-1773.
- (18) For the X-ray structure of a cobaltacyclopentadiene(alkyne) species see: Dosa, P.I.; Whitener, G.D.; Vollhardt, K.P.C.; Bond, A.D.; Teat, S.J. Cobalt-mediated synthesis of angular [4]phenylene: structural characterization of a metallacyclopentadiene(alkyne) intermediate and its thermal and photochemical conversion. *Org. Lett.* **2002**, *4*, 2075-2078.
- (19) Zhao, Y.; Liu, Y.; Bi, S.; Liu, Y. Theoretical investigation on the regioselectivity of Ni(COD)₂-catalyzed [2+2+2] cycloaddition of unsymmetric diynes and CO₂. *J. Organomet. Chem.* **2014**, *758*, 45-54.
- (20) A blank experiment was run in the case of the cyclotrimerisation of phenylacetylene using [Rh(COD)₂]BF₄ without BIPHEP but only decomposition of the starting acetylene was observed demonstrating the need of the ligand in such a process.
- (21) Hansch, C.; Leo, A.; Taft R. W. Survey of Hammett Substituent Constants and Field Parameters. *Chem. Rev.* **1991**, *91*, 165-195.
- (22) a) Becke, A.D. Density-functional thermochemistry. III. The role of exact exchange. *J. Chem. Phys.* **1993**, *98*, 5648-5652; b) Lee, C.; Yang, W.; Parr, R.G. Development of the Colle-Salvetti correlation-energy formula into a functional of the electron density. *Phys. Rev. B* **1988**, *37*, 785-789; c) Stephens, P.J.; Devlin, F.J.; Chabalowski, C.F.; Frisch, M.J. Ab Initio calculation of vibrational absorption and circular dichroism spectra using density functional force fields. *J. Phys. Chem.* **1994**, *98*, 11623-11627.
- (23) Frisch, M.J.; Trucks, G.W.; Schlegel, H.B.; Scuseria, G.E.; Robb, M.A.; Cheeseman, J.R.; Scalmani, G.; Barone, V.; Mennucci, B.; Petersson, G.A.; Nakatsuji, H.; Caricato, M.; Li, X.; Hratchian, H.P.; Izmaylov, A.F.; Bloino, J.; Zheng, G.; Sonnenberg, J.L.; Hada, M.; Ehara, M.; Toyota, K.; Fukuda, R.; Hasegawa, J.; Ishida, M.; Nakajima, T.; Honda, Y.; Kitao, O.; Nakai, H.; Vreven, T.; Montgomery Jr. J.A.; Peralta, J.E.; Ogliaro, F.; Bearpark, M.; Heyd, J.J.; Brothers, E.; Kudin, K.N.; Staroverov, V.N.; Kobayashi, R.; Normand, J.; Raghavachari, K.; Rendell, A.; Burant, J.C.; Iyengar, S.S.; Tomasi, J.; Cossi, M.; Rega, N.; Millam, J.M.; Klene, M.; Knox, J.E.; Cross, J.B.; Bakken, V.; Adamo, C.; Jaramillo, J.; Gomperts, R.; Stratmann, R.E.; Yazyev, O.; Austin, A.J.; Cammi, R.; Pomelli, C.; Ochterski, J.W.; Martin, R.L.; Morokuma, K.; Zakrzewski, V.G.; Voth, G.A.; Salvador, P.; Dannenberg, J.J.; Dapprich, S.; Daniels, A.D.; Farkas, Ö.; Foresman, J.B.; Ortiz, J.V.; Cioslowski, J.; Fox, D.J. Gaussian 09, Revision E.01; Gaussian, Inc.: Pittsburgh, PA, **2009**.
- (24) Grimme, S.; Antony, J.; Ehrlich, S.; Krieg, H. A consistent and accurate ab initio parametrization of density functional dispersion correction (DFT-D) for the 94 elements H-Pu. *J. Chem. Phys.* **2010**, *132*, 154104.
- (25) a) Becke, A.D.; Johnson, E.R. A density-functional model of the dispersion interaction. *J. Chem. Phys.* **2005**, *123*, 154101; b) Johnson, E.R.; Becke, A.D. A post-Hartree-Fock model of intermolecular interactions. *J. Chem. Phys.* **2005**, *123*, 024101.
- (26) a) Dunning Jr. T.H. Gaussian basis sets for use in correlated molecular calculations. I. The atoms boron through neon and hydrogen. *J. Chem. Phys.* **1989**, *90*, 1007-1023; b) Woon, D.E.; Dunning Jr. T.H. Gaussian basis sets for use in correlated molecular calculations. III. The atoms aluminum through argon. *J. Chem. Phys.* **1993**, *98*, 1358-1371.
- (27) Peterson, K.A.; Figgen, D.; Dolg, M.; Stoll, H. Energy-consistent relativistic pseudopotentials and correlation consistent basis sets for the 4d elements Y-Pd. *J. Chem. Phys.* **2007**, *126*, 124101.
- (28) Jover, J. Quantitative DFT modeling of product concentration in organometallic reactions: Cu-mediated pentafluoroethylation of benzoic acid chlorides as a case study. *Phys. Chem. Chem. Phys.* **2017**, *19*, 29344-29353.
- (29) Atkins, P.; De Paula, J. in *Physical Chemistry*, Oxford University Press, Oxford, **2006**.
- (30) a) Strajbl, M.; Sham, Y.Y.; Villà, J.; Chu, Z.-T.; Warshel, A. Calculations of activation entropies of chemical reactions in solution. *J. Phys. Chem. B*, **2000**, *104*, 4578-4584; b) Cooper, J.; Ziegler, T. A density functional study of S_N2 substitution at square-planar platinum(II) complexes. *Inorg. Chem.* **2002**, *41*, 6614-6622; c) Yu, Z.-X.; Houk, K.N. Intramolecular 1,3-dipolar ene reactions of nitrile oxides occur by stepwise 1,1-cycloaddition/retro-ene mechanisms. *J. Am. Chem. Soc.* **2003**, *125*, 13825-13830; d) Leung, B.O.; Reid, D.L.; Armstrong, D.A.; Rauk, A. Entropies in solution from entropies in the gas phase. *J. Phys. Chem. A*, **2004**, *108*, 2720-2725; e) Xia, Y.; Liang, Y.; Chen, Y.; Wang, M.; Jiao, L.; Huang, F.; Liu, S.; Li, Y.; Yu, Z.-X. An unexpected role of a trace amount of water in catalyzing proton transfer in phosphine-catalyzed (3+2) cycloaddition of allenolates and alkenes. *J. Am. Chem. Soc.* **2007**, *129*, 3470-3471.
- (31) a) Mennucci, B.; Cammi, R.; Tomasi, J. Medium effects on the properties of chemical systems: electric and magnetic response of donor-acceptor systems within the polarizable continuum model. *Int. J. Quantum Chem.*, **1999**, *75*, 767-781; b) Tomasi, J.; Mennucci, B.; Cammi, R. Quantum mechanical continuum solvation models. *Chem. Rev.*, **2005**, *105*, 2999-3094.
- (32) a) Kelly, C.P.; Cramer, C.J.; Truhlar, D.G. SM6: A density functional theory continuum solvation model for calculating aqueous solvation free energies of neutrals, ions, and solute-water clusters. *J. Chem. Theory. Comput.* **2005**, *1*, 1133-1152; b) Kelly, C.P.; Cramer, C.J.; Truhlar, D.G. Aqueous solvation free energies of ions and ion-water clusters based on an accurate value for the absolute aqueous solvation free energy of the proton. *J. Phys. Chem. B* **2006**, *110*, 16066-16081; c) Bryantsev, V.S.; Diallo, M.S.; Goddard III, W.A. Calculation of solvation free energies of charged solutes using mixed cluster/continuum models. *J. Phys. Chem. B*, **2008**, *112*, 9709-9719.
- (33) Gonzalez, C.; Schlegel, H.B. An improved algorithm for reaction path following. *J. Chem. Phys.* **1989**, *90*, 2154-2161.

Graphic entry for the Table of Contents (TOC):

